Smart Mater. Struct. **19** (2010) 035004 (13pp) doi:10.1088/0964-1726/19/3/035004

Analysis of piezoelectric laminates by generalized finite element method and mixed layerwise-HSDT models

D A F Torres and P T R Mendonça

Group of Mechanical Analysis and Design—GRANTE, Department of Mechanical Engineering, Federal University of Santa Catarina, 88040-900, Florianópolis, SC, Brazil

E-mail: diego.amadeu@gmail.com and mendonca@grante.ufsc.br

Received 16 April 2009, in final form 7 December 2009
Published 22 January 2010
Online at stacks.iop.org/SMS/19/035004

Abstract

This paper presents a procedure to numerically analyze the coupled electro-structural response of laminated plates with orthotropic fiber reinforced layers and piezoelectric layers using the generalized finite element method (GFEM). The mechanical unknowns, the displacements, are modeled by a higher order shear deformation theory (HSDT) of the third order, involving seven generalized displacement functions. The electrical unknowns, the potentials, are modeled by a layerwise theory, utilizing piecewise linear functions along the thickness of the piezoelectric layers. All fields are enriched in the in-plane domain of the laminate, according to the GFEM, utilizing polynomial enrichment functions, defined in global coordinates, applied on a bilinear partition of unities defined on each element. The formulation is developed from an extended principle of Hamilton and results in a standard discrete algebraic linear motion equation. Numerical results are obtained for some static cases and are compared with several numerical and experimental results published in the literature. These comparisons show consistent and reliable responses from the formulation. In addition, the results show that GFEM meshes require the least number of elements and nodes possible for the distribution of piezoelectric patches and the enrichment provides more flexibility to reproduce the deformed shapes of adaptive laminated plates.

1. Introduction

Smart/intelligent structures have received increasing attention from researchers in recent decades due to several aspects. The motivation for utilizing adaptive materials is to enable a structure to change its shape or its material/structural properties, thereby improving performance and service life.

Electrostrictive materials, magnetostrictive materials, shape memory alloys, magneto- or electro-rheological fluids, polymer gels, and piezoelectric materials, for example, can all be used to design and develop structures that can be called smart.

These adaptive materials can reduce the need for complex mechanical linkages and actuator systems since the adaptive material itself is integrated (embedded/bonded) within the structure, resulting in the reduction of weight and avoiding some problems inherent to these mechanical devices (Chee *et al* 1998).

Piezoelectric materials can be applied in laminated composite structures as patches and films or to form layers within of the laminate. Because they exhibit coupled mechanical–electrical behavior, they can be used as sensors, measuring strains and accelerations, or as actuators, when electric potentials are applied to generate a field of deformations in the structure.

In the past three decades, a large variety of models have been developed to predict the behavior of piezoelectric materials in smart structures. These models may be classified into three different categories: induced strain models, coupled electromechanical models and coupled thermo-electromechanical models.

The coupled electromechanical models provide a more consistent representation of both the active and sensitive responses of piezoelectric materials through the incorporation of both mechanical displacements and electric potentials as state variables in the formulation. The coupled

electromechanical models are most commonly implemented in finite element codes. The early codes were modeled with solid elements, following the pioneering work of Allik and Hughes (1970). However, the hexahedron or brick elements display excessive shear stiffness as the element thickness decreases. This problem was circumvented by adding three incompatible internal degrees of freedom to the element (Detwiler *et al* 1995). Other formulations based on solid elements have been developed, (see, for instance, Tzou and Tseng (1990) and Ha *et al* (1992)), but, as a rule, the completely three-dimensional modeling of laminated piezoelectric structures results in systems with a large number of degrees of freedom, since they require one solid element per layer of the laminate.

One strategy to reduce the cost associated with the full solid element models is in the use of a layerwise theory (LT) to describe both mechanical and electrical unknowns. Among others, Saravanos *et al* (1997) can be cited as a reference for the complete dynamic electromechanical response of smart piezoelectric plates under external mechanical or electric loading. Lee (2001) presents a complete family of finite elements for beams, plates and shells based on LT for all state variables. Lage *et al* (2004), also incorporated the coupled magneto-electro-elastic phenomenon in a partially hybrid functional with higher order functions along the thickness. A more elaborate strategy is developed by Cotoni *et al* (2006), who presents a finite element formulation based on a fourth order expansion through the laminate thickness, combined with a piecewise linear term to describe the mechanical variables and a quadratic distribution of the electric potential inside each piezoelectric layer.

The layerwise theories still involve a large number of degrees of freedom in the models, similar in extent to the full solid elements. This inconvenience induced the parallel development of two-dimensional models. The most simple of these are based on the classical laminated plate theory (CLPT), for instance, the work of Hwang and Park (1993), who developed a two-dimensional quadrilateral plate element with one electrical degree of freedom per piezoelectric layer per element. The output voltage was post-processed from the direct piezoelectric equation.

The simple CLPT offers poor kinematic approximation capabilities for a complex laminate system, such as those equipped with piezoelectric patches. Therefore, models based on the first order shear deformation theory (FSDT) were tested, such as that described by Detwiler *et al* (1995), for the linear response of coupled electrical-mechanical behavior, or by Gao and Shen (2003), who considered the geometrical non-linearity of the structure.

The particular structural configuration of a laminate with piezoelectric layers or patches makes it very difficult to adequately model using a single equivalent layer kinematic model, applied to both mechanical and electrical unknowns. Therefore, a sensible strategy involves the use of a single equivalent layer model for the mechanical unknowns and a layerwise theory for the electric potential. Some of the most simple of these combinations are those using the FSDT for the mechanical displacements and LT for the potential, for example, the shell element formulated by Saravanos (1997). Cen *et al* (2002) have also employed a partially hybrid energy functional for correcting the transverse shear deformation in their mixed FSDT–LT finite element formulation. In a different manner, Liew *et al* (2004) utilized the mixed FSDT–LT models in a formulation based on the element-free Galerkin method.

It is well known that the FSDT results in some deficiencies in the approximation of the mechanical response of anisotropic laminates, particularly in the form of underestimated displacements and poor transverse shear stresses. A higher order shear deformation theory (HSDT) behaves much better and several studies indicate that it is a good choice for the mechanical displacements in an piezoelectric laminate, combined with the LT for the electric potential. This can be seen in the work of Reddy (1999), Chee (2000) and Faria (2006), among others.

This paper presents a procedure to numerically analyze the coupled electro-structural response of laminated plates with orthotropic fiber reinforced layers and piezoelectric layers, by the generalized finite element method (GFEM). The mechanical unknowns, the displacements, are modeled by an HSDT of the third order. The electrical unknowns, the potentials, are modeled by a layerwise theory, utilizing piecewise linear functions along the thickness of the piezoelectric layers. All fields are enriched according to the GFEM, utilizing polynomial enrichment functions applied on a bilinear partition of unity defined on each element. The remainder of this paper is outlined as follows: section 2 reviews the basics of GFEM. Section 3 deals with the linear electro-elasticity formulation. Section 4 details the proposed application of the GFEM strategy to the problem of laminated plates with orthotropic piezoelectric layers, showing the discretization, the global enrichment of the approximating spaces, stiffness and inertia matrices, mechanical–electrical coupling matrices and mechanical and electric dynamic load vectors. Section 5 shows numerical applications for the static analysis of classical models of adaptive plates comparing the results of the present formulation with those in the literature, and section 6 gives some conclusions.

2. Generalized finite element method

Oden *et al* (1998) presented a hybrid method combining the *hp* clouds method and the conventional form of the finite element method. This strategy takes into account the idea of adding hierarchical refinements to a set of shape functions associated to finite elements, such as the Lagrangian interpolation functions which satisfy the requirement of a partition of unity (PoU). The method became consolidated with the works of Duarte *et al* (2000), Strouboulis *et al* (2000) and Strouboulis *et al* (2001), resulting in the methodology called generalized finite element method (GFEM).

In the GFEM context, discrete spaces for a Galerkin method are defined using the concept of the partition of unit finite element method (PUFEM), of Babuška *et al* (1994), Melenk (1995), Melenk and Babuška (1996), and Babuška and Melenk (1997) and of the *hp* clouds method of Duarte (1996) and Duarte and Oden (1996). A mesh of elements is created to: (a) facilitate the numerical integration; and (b)

define the PoU locally within elements by intrinsic coordinates. Finally, the PoU functions are enriched by functions defined in global coordinates. This last aspect is responsible for the high efficiency of the method. Usually the enrichment functions are polynomials, but special enrichment functions can be used to provide more accurate and robust simulations. These functions can be built based on *a priori* knowledge of the solution of a problem as well as based on the solution of local boundary value problems.

In recent years, the GFEM has been applied to a diversity of phenomena such as the analysis of dynamic crack propagation (Duarte *et al* 2001) and porous materials (Strouboulis *et al* 2001, 2003). It has also been used to build arbitrarily smooth approximations for handling higher order distributional boundary conditions (Duarte *et al* 2006). Barros *et al* (2007) uses it to perform p-adaptive analysis and error estimation. O'Hara (2007) and O'Hara *et al* (2009) use GFEM to analyze multiscale phenomena. Barcellos *et al* (2009) develops a C^k continuous finite element formulation for the Kirchhoff laminate model. A procedure to define richer approximate subspaces for shell structures and the treatment of the boundary layer phenomenon is addressed by Garcia *et al* (2009).

Partition of unity (PoU) is a set of functions where, among other properties (see Oden and Reddy 1976), the sum of their values is equal to unity on every point of the support. It can be noted that the standard finite element shape functions form a partition of unity. In general, the GFEM can be briefly defined as a strategy to enlarge the FEM approximation space by adding special functions to the conventional approximation basis. This basis now takes the role of a partition of unity and allows inter-element continuity and creates conforming approximations. The enrichment allows the application of any information that reflects previous knowledge of the boundary value problem solution, such as a singular function resulting from local asymptotic expansion of the exact solution close to a point. The approximating capabilities of the enrichment functions are included in the function space of the method while keeping the same standard structure of an FEM code.

The construction of the method can be summarized as follows. Initially, a cloud family is defined by

$$\mathcal{F}_N^{k,p} = \{\{\varphi_j(\mathbf{x})\}_{j=1}^N \bigcup \{\varphi_j(\mathbf{x})\mathcal{L}_{ji}(\mathbf{x})\}_{j=1}^N | i \in \jmath(j)\} \qquad (1)$$

where $\varphi_j(\mathbf{x})$ are PoU functions and $\mathcal{L}_{ji}(\mathbf{x})$ are the enrichment functions, both related to the node j, and $\jmath(j)$ is an index set which refers to the enrichment functions associated with each node. In this definition, the cloud family functions $\mathcal{F}_N^{k,p}$ comprise the PoU, which generates the polynomial space of degree k, $\mathcal{P}_k$, which is able to represent, in an exact form, polynomials of the space of degree p, $\mathcal{P}_p$. This cloud family is used to build the following approximation functions for an arbitrary displacement component $u(\mathbf{x})$

$$\tilde{u}(\mathbf{x}) = \sum_{j=1}^{N} \varphi_j(\mathbf{x}) \left\{ u_j + \sum_{i=1}^{q_j} \mathcal{L}_{ji}(\mathbf{x}) b_{ji} \right\} = \mathbf{\Phi}^{\mathrm{T}}\mathbf{U} \qquad (2)$$

with

$$\mathbf{U}^{\mathrm{T}}(\mathbf{x}) = [\, u_1 \quad b_{1_1} \quad \cdots \quad b_{1_{q_j}} \quad \cdots \quad \cdots \quad u_N \quad b_{N_1} \quad \cdots \quad b_{N_{q_j}} \,] \qquad (3)$$

where u_i and $b_{i_{q_j}}$ are the nodal parameters associated with the standard finite element shape functions $\varphi_j(\mathbf{x})$ and enriched functions $\varphi_j(\mathbf{x})\mathcal{L}_{ji}(\mathbf{x})$, respectively. The complete set of functions can be grouped in vector form as

$$\mathbf{\Phi}^{\mathrm{T}} = [\, \varphi_1 \quad \mathcal{L}_{1_1}\varphi_1 \quad \cdots \quad \mathcal{L}_{1_{q_j}}\varphi_1 \quad \cdots \quad \cdots \quad \varphi_N \quad \mathcal{L}_{N_1}\varphi_N \quad \cdots \quad \mathcal{L}_{N_{q_j}}\varphi_N \,] \qquad (4)$$

where q_j is the number of enrichment functions of each node.

Let $\mathscr{U}$ and $\mathscr{V} \in \mathcal{H}^1(\Omega)$ be Hilbert spaces of degree 1 defined on the domain Ω and consider the following boundary value problem: find $u \in \mathscr{U}$ such that $\mathscr{B}(u, v) = \mathscr{L}(v), \forall\, v \in \mathscr{V}$. Let $\mathscr{U}_h$ be the subspace spanned by a set of kinematically admissible functions and $\mathscr{V}_h$ the subspace spanned by a set of kinematically admissible variations. We define the following Galerkin approximation for the boundary value problem using the GFEM approach: find $\tilde{u} \in \mathscr{U}_h$ such that $\mathscr{B}(\tilde{u}, \tilde{v}) = \mathscr{L}(\tilde{v})$, $\forall\, \tilde{v} \in \mathscr{V}_h$, where $\tilde{u}$ and $\tilde{v} \in \mathscr{U}_h = \mathscr{V}_h \subset \mathcal{H}^1$, $\mathcal{H}^1$ being the Hilbert space of degree 1 defined on the domain Ω. $\mathscr{B}(\bullet, \bullet)$ is a bilinear form of $\mathcal{H}^1 \times \mathcal{H}^1 \longrightarrow \mathbb{R}$ and $\mathscr{L}(\bullet)$ is a linear form of $\mathcal{H}^1 \longrightarrow \mathbb{R}$. The formulation leads to the equation system $\mathscr{B}(\mathbf{\Phi}^{\mathrm{T}}\mathbf{U}, \mathbf{\Phi}^{\mathrm{T}}\mathbf{V}) = \mathscr{L}(\mathbf{\Phi}^{\mathrm{T}}\mathbf{V})$ where

$$\mathbf{V}^{\mathrm{T}} = [\, v_1 \quad c_{1_1} \quad \cdots \quad c_{1_{q_j}} \quad \cdots \quad \cdots \quad v_N \quad c_{N_1} \quad \cdots \quad c_{N_{q_j}} \,] \qquad (5)$$

are nodal parameters related to the test function, such that $\mathbf{\Phi}^{\mathrm{T}}\mathbf{V} \in \mathscr{V}_h$. In cases where the enrichment functions $\mathcal{L}_{ij}$ are polynomials, the proximation $\tilde{u}$ will be represented in the following particular form

$$u_p(\mathbf{x}) = \sum_{j=1}^{N} \varphi_j(\mathbf{x}) \left\{ u_j + \sum_{i=1}^{q_{j(p)}} p_{ji}(\mathbf{x}) b_{ji} \right\} = \mathbf{\Phi}^{\mathrm{T}}\mathbf{U}. \qquad (6)$$

The present implementation of a GFEM formulation for plates is performed with enrichment polynomials up to the third degree, applied on a PoU defined by bilinear shape functions, according to the following linear combination

$$\varphi_j \times \left\{ 1, \frac{x - x_j}{h_{x_j}}, \frac{y - y_j}{h_{y_j}}, \left(\frac{x - x_j}{h_{x_j}}\right)^2, \left(\frac{x - x_j}{h_{x_j}}\right)\left(\frac{y - y_j}{h_{y_j}}\right), \ldots, \left(\frac{y - y_j}{h_{x_j}}\right)^3 \right\} \qquad (7)$$

where $\bar{x} = (x - x_j)/h_{xj}$ and $\bar{y} = (y - y_j)/h_{xj}$ are normalized coordinates. φ_j, $j = 1, 2, \ldots, N$ are standard finite element bilinear shape functions, $\mathbf{x}_j = (x_j, y_j)$ are nodal coordinates of an arbitrary node j. h_{x_j} and h_{y_j} are the cloud characteristic dimensions of the node in the directions x and y, respectively, and N is the number of nodes of the finite element mesh. It can be noted that using this procedure of enrichment only the partition of unity keeps its interpolator characteristic—the enriched functions associated with a given node are zero there, and, therefore, they are not interpolation functions in the classical sense. Only the PoU satisfies the Kronecker delta condition, i.e., $\varphi_j(x_i) = \delta_{ij}$. Therefore,

the Dirichlet boundary conditions cannot be directly imposed, making special procedures necessary to impose them. One efficient procedure to impose these conditions is through the so-called boundary functions, as developed by Garcia (2003) and Garcia *et al* (2009).

3. Linear electro-elasticity

Most models of piezoelectric materials used as sensors and actuators in intelligent structures consider only the linear piezoelectric constitutive equation, $D_i = \varepsilon_{ij} E_j$, which is partly developed from electromagnetic theory. However, this is only true for a homogeneous and isotropic dielectric material, for which it is assumed that the polarization (**P**) of the dielectric material is linearly proportional to the electric field (**E**).

According to Reddy (2004), the coupling between the mechanical, thermal and electric fields can be established employing thermodynamic principles and the Maxwell relations. Analogously to the deformation energy functional U_0 in the linear elasticity theory and to the free energy functional of Helmholtz Ψ_0 in thermoelasticity, the existence of a functional Φ_0 is assumed such that

$$\Phi_0(\varepsilon_{ij}, E_i, \theta) = U_0 - \mathbf{E}\cdot\mathbf{D} - \eta\theta = \tfrac{1}{2}C_{ijkl}\varepsilon_{ij}\varepsilon_{kl} - e_{ijk}\varepsilon_{ij}E_k - \beta_{ij}\varepsilon_{ij}\theta - \frac{1}{2}\chi_{kl}E_kE_l - p_kE_k\theta - \frac{\rho c_v}{2\theta_0}\theta^2 \tag{8}$$

denominated the Gibbs free energy functional, or the enthalpy functional, where η is the enthalpy, C_{ijkl} are elastic moduli, e_{ijk} are the piezoelectric moduli or, more precisely, the constants of piezoelectric deformation, χ_{ij} are dielectric constants, p_k are the pyroelectric constants, β_{ij} are thermal expansion coefficients, c_v is the specific heat at constant volume, per unit mass, and θ_0 is the reference temperature. Differentiation of this functional with respect to the fields $\boldsymbol{\varepsilon}$, **E** and θ results in the coupled constitutive relations for a deformable pyro-piezoelectric material, as can be seen in Reddy (2004).

The formulation utilized in the present paper ignores variations in temperature, such that the coupled equations become

$$\sigma_i = C_{ij}^E\varepsilon_j - e_{ik}E_k \qquad D_k = e_{kj}\varepsilon_j + \chi_{kl}^{\varepsilon}E_l \qquad \eta = \beta_j\varepsilon_j + p_kE_k \tag{9}$$

where σ_{ij} are the components of the mechanical stress tensor, D_i are the components of the electric displacement vector and η is the enthalpy. In (9) the contracted notation was used, considering the stress and strain tensors to be symmetrical. The enthalpy becomes uncoupled from the other fields, and the problem solution is obtained from the first two equations. These relations can be reordered into one single-matrix linear relation, electromechanically coupled, in the orthotropic material directions, along axes 1, 2 and 3

$$\begin{Bmatrix} \boldsymbol{\sigma}^1 \\ \mathbf{D}^1 \end{Bmatrix}^k = \begin{bmatrix} \mathbf{C}^1 & -\mathbf{e}^{1^{\mathrm{T}}} \\ \mathbf{e}^1 & \boldsymbol{\chi}^1 \end{bmatrix}^k \begin{Bmatrix} \boldsymbol{\varepsilon}^1 \\ \mathbf{E}^1 \end{Bmatrix}^k. \tag{10}$$

The superscript 1 indicates the coordinate system and k is the number of an arbitrary piezoelectric layer. For the piezoelectric extensional mode of actuation, only the following coefficients in (10) are different to zero: C_{11}^1, C_{12}^1, C_{13}^1, C_{22}^1, C_{23}^1, C_{33}^1, C_{44}^1, C_{55}^1 and C_{66}^1, for the stiffness matrix; e_{15}^1, e_{24}^1, e_{31}^1, e_{32}^1 and e_{33}^1, for the piezoelectric matrix; and χ_{11}^1, χ_{22}^1 and χ_{33}^1, for the dielectric matrix.

In this formulation each composite layer is considered orthotropic, whether it is piezoelectric or not. Therefore, the constitutive relation (10) must be rotated to the global laminate coordinate system, according to the layer orientation angle, and then be combined into the laminate constitutive relation.

In addition, for simple monolithic piezoelectric materials polarized along the principal transverse direction 3, the piezoelectric properties would be the same in both the 1 and 2 in-plane directions. The two piezoelectric constants that are usually tabulated are d_{31} and d_{33} (in the strain formulation)—the first subscript indicates the direction of the electric field and the second subscript the direction of the strain. It can be shown that the material parameters are interrelated as follows

$$e_{ik} = d_{ij}C_{jk}. \tag{11}$$

4. Discrete formulation of the GFEM

In this study a generalized finite element is implemented to model laminated plates with piezoelectric sensors and actuators. The domain is divided into quadrilateral elements defined by 8 nodes and the corresponding standard biquadratic serendipity functions. The partition of unity is defined by the nodes of the four vertices and the corresponding Lagrangian bilinear functions, which are, in turn, enriched according to the GFEM procedure in order to generate the enriched space of approximation for the unknown electrical and mechanical fields.

The formulation developed here is derived from Hamilton's principle, which is constructed in such a way that it is a variational equivalent to the differential governing equations of the mechanical and electrical responses in a continuum electromechanically coupled (Lee 2001). These equations are Cauchy's equations of motion,

$$\frac{\partial\sigma_{ij}}{\partial x_j} + f_i = \rho\ddot{u}_i \tag{12}$$

(where the summation convention is used) and Maxwell's equations of conservation of electric flux

$$\frac{\partial D_i}{\partial x_i} = \mathbf{Q} \tag{13}$$

where σ_{ij} are the Cartesian components of the stress tensor, f_i are the components of body force per unit volume, ρ is the specific mass per unit volume of the material, u_i are the components of mechanical displacement, D_i are the components of electric displacement (electric flux) and q is the electric charge.

The functional of Hamilton's principle is (Chee 2000)

$$\int_{t_0}^{t_1} (\delta K - \delta P + \delta W)\,\mathrm{d}t = 0 \tag{14}$$

which must hold for any $t_1 > t_0$, where K, P and W are the total kinetic energy, the total potential deformation energy and the total work of external forces applied to the system, respectively, and δ is the variation operator. The expression can be expanded as

$$\int_{t_0}^{t_1}\left\{-\int_V \rho\delta\mathbf{u}^{\mathrm{T}}\ddot{\mathbf{u}}(\mathbf{x},t)\,\mathrm{d}V-\int_V\begin{Bmatrix}\boldsymbol{\sigma}^x\\ \mathbf{D}^x\end{Bmatrix}^{\mathrm{T}}\begin{Bmatrix}\delta\boldsymbol{\epsilon}^x\\ -\delta\mathbf{E}^x\end{Bmatrix}\mathrm{d}V + \int_V\delta\mathbf{u}^{\mathrm{T}}\mathbf{b}^V\,\mathrm{d}V+\int_S\delta\mathbf{u}^{\mathrm{T}}\mathbf{f}^S\,\mathrm{d}S+\delta\mathbf{u}^{\mathrm{T}}\mathbf{f}^P + \int_V\delta\varphi^{\mathrm{T}}\mathbf{Q}\,\mathrm{d}V-\int_S\delta\varphi^{\mathrm{T}}\mathbf{q}\,\mathrm{d}S\right\}\mathrm{d}t=0 \tag{15}$$

where $\mathbf{u}$ is the vector of mechanical displacement, $\boldsymbol{\sigma}$ is the stress tensor, $\boldsymbol{\varepsilon}$ is the strain tensor, $\mathbf{D}$ is the electric displacement, $\mathbf{E}$ is the electric field, $\mathbf{f}^S$ is the surface force, $\mathbf{f}^V$ is the body force, $\mathbf{f}^P$ are concentrated forces, φ is the electric potential, $\mathbf{Q}$ is a free electric charge and $\mathbf{q}$ is a free electric charge at the surface. (The components of the stress and strain tensors appear in the equation organized in vector form.)

The mechanical behavior of the plate undergoing bending is modeled by the equivalent single layer (ESL) methodology, using the kinematical hypothesis following Levinson's higher order shear deformation theory (Levinson 1980). Hence, the present formulation is based on the following assumed displacement field

$$\begin{aligned}u(\mathbf{x},t)&=u^0(x,y,t)+z\psi_x(x,y,t)+z^3\psi_{3x}(s,y,t)\\ v(\mathbf{x},t)&=v^0(x,y,t)+z\psi_y(x,y,t)+z^3\psi_{3y}(x,y,t)\\ w(\mathbf{x},t)&=w^0(x,y,t)\end{aligned} \tag{16}$$

where (u, v, w) are the components, in Cartesian directions, of the displacement of an arbitrary point in the laminated plate. This theory is chosen here due its relatively lower computational cost, since only seven generalized displacements are required, u^0, v^0, w^0, ψ_x, ψ_y, ψ_{3x} and ψ_{3y}. u^0, v^0 and w^0 are the displacements of a point in the reference plane, ψ_x and ψ_y are rotations of a segment normal to the middle plane around the y-axis and x-axis, respectively, and ψ_{3x} and ψ_{3y} are higher order warping variables in the x–z and y–z-planes, respectively. These are the mechanical unknown fields that can be approximated over the bi-dimensional (x, y) domain through function spaces with C^0 regularity.

Opting for a thin or thick plate model is a decision which cannot be made *a priori* because it depends on the solution and the computation goals, for example, displacements or stresses. Moreover, according to Szabó and Babuška (1991), hierarchic plate/shell models $(HM|i)$ have the property

$$\lim_{i\to\infty}\|u_{EX}^{3\mathrm{D}}-u_{EX}^{(HM|i)}\|_{E(\Omega)}\leqslant Cd^{\alpha_i} \tag{17}$$

when $u_{EX}^{3\mathrm{D}}$, the fully three-dimensional solution, is smooth. In (17), C is a constant, independent of i, the model order, α_i is a constant which is dependent on i, and $\alpha_{i+1} > \alpha_i$. Thus, the HSDT has a higher rate of convergence than the FSDT or CLPT.

Using the linear strain–displacement relations it is possible to obtain the strain field, which is separated into *coplanar strains* $\boldsymbol{\varepsilon}_{mf}(\mathbf{x},t)$

$$\begin{aligned}\boldsymbol{\varepsilon}_{mf}(\mathbf{x},t)&=\begin{Bmatrix}\varepsilon_x(\mathbf{x},t)\\ \varepsilon_y(\mathbf{x},t)\\ \gamma_{xy}(\mathbf{x},t)\end{Bmatrix}\\ &=\begin{Bmatrix}\frac{\partial u^0(x,y,t)}{\partial x}\\ \frac{\partial v^0(x,y,t)}{\partial y}\\ \frac{\partial u^0(x,y,t)}{\partial y}+\frac{\partial v^0(x,y,t)}{\partial x}\end{Bmatrix}+z\begin{Bmatrix}\frac{\partial\psi_x(x,y,t)}{\partial x}\\ \frac{\partial\psi_y(x,y,t)}{\partial y}\\ \frac{\partial\psi_x(x,y,t)}{\partial y}+\frac{\partial\psi_y(x,y,t)}{\partial x}\end{Bmatrix}\\ &\quad+z^3\begin{Bmatrix}\frac{\partial\psi_{3x}(x,y,t)}{\partial x}\\ \frac{\partial\psi_{3y}(x,y,t)}{\partial y}\\ \frac{\partial\psi_{3x}(x,y,t)}{\partial y}+\frac{\partial\psi_{3y}(x,y,t)}{\partial x}\end{Bmatrix}\end{aligned} \tag{18}$$

where it is possible identify the *generalized extensional strains*, $\boldsymbol{\varepsilon}^0$, the *generalized flexural rotations*, $\boldsymbol{\kappa}_1$, and the *generalized warp rotations*, $\boldsymbol{\kappa}_3$, such that

$$\boldsymbol{\varepsilon}_{mf}(\mathbf{x},t)=\boldsymbol{\varepsilon}^0(x,y,t)+z\boldsymbol{\kappa}_1(x,y,t)+z^3\boldsymbol{\kappa}_3(x,y,t). \tag{19}$$

The *transverse shear strains*, $\boldsymbol{\gamma}_c(\mathbf{x},t)$, are given by

$$\begin{aligned}\boldsymbol{\gamma}_c(\mathbf{x},t)&=\begin{Bmatrix}\gamma_{yz}(\mathbf{x},t)\\ \gamma_{xz}(\mathbf{x},t)\end{Bmatrix}\\ &=\begin{Bmatrix}\psi_y(x,y,t)+\frac{\partial w^0(x,y,t)}{\partial y}\\ \psi_x(x,y,t)+\frac{\partial w^0(x,y,t)}{\partial x}\end{Bmatrix}+3z^2\begin{Bmatrix}\psi_{3y}(x,y,t)\\ \psi_{3x}(x,y,t)\end{Bmatrix}\end{aligned} \tag{20}$$

where it is possible identify the *generalized shear strains*, $\boldsymbol{\gamma}^0$, and the *generalized shear-warp strains*, $\boldsymbol{\kappa}_2$, such that

$$\boldsymbol{\gamma}_c=\boldsymbol{\gamma}^0+3z^2\boldsymbol{\kappa}_2. \tag{21}$$

At this stage it is necessary to define how the electric degrees of freedom are incorporated. Reddy's layerwise theory (Reddy 2004) is adopted here for interpolation of the electric potential field. The electric potential in the element, $\varphi(\mathbf{x},t)$, is approximated by piecewise functions along thicknesses of the piezoelectric layers. This hypothesis is acceptable since the voltage is generally applied perpendicular to the active layers, and assuming homogeneous material.

According to these laminate theories, each layer is modeled using independent approximations for the in-plane displacement components and the electrostatic potential in a unified representation, in accordance with the linear theory of piezoelectricity.

Consider a laminate with n_{piez} piezoelectric layers. $N = n_{\mathrm{piez}}+1$ electric potential nodal values, φ_{no}^1 to φ_{no}^N, corresponds to each arbitrary node *no* on the laminate middle plane if such piezoelectric layers are contiguous, or $N = 2n_{\mathrm{piez}}$ electric potential nodal values if there is inert material between them. Hence the potential approximation $\tilde{\varphi}_{no}$ in an intermediate position z within an arbitrary piezoelectric layer k at an instant t is given by the expression

$$\tilde{\varphi}_{no}(z,t)^k=\varphi_{no}^{k-1}(t)\zeta_{k-1}+\varphi_{no}^k(t)\zeta_k \tag{22}$$

with

$$\zeta_{k-1}=\left(\frac{z_k-z}{h_k}\right)\qquad\text{and}\qquad\zeta_k=\left(\frac{z-z_{k-1}}{h_k}\right). \tag{23}$$

The GFEM formulation is implemented beginning with the definition of the partition of unity (PoU) over the

element domain. The enrichment is carried out by adding new parameters linked to unknown nodal values which are associated with the functions that multiply the original base functions. In this way, the generalized mechanical displacements over the laminate middle plane, $(u^0, v^0, w^0, \psi_x, \psi_y, \psi_{3x}, \psi_{3y})$, can be approximated, for example, as

$$\tilde{u}^0 = \sum_{no=1}^{Nne} \mathbb{N}^e_{no}(x,y)\left(u^0_{no}(t) + \sum_{j=1}^{nf(u^0_{no})} u^{0^j}_{no}(t)\, f^j_{u^0_{no}}(x,y)\right)$$

$$\tilde{v}^0 = \sum_{no=1}^{Nne} \mathbb{N}^e_{no}(x,y)\left(v^0_{no}(t) + \sum_{j=1}^{nf(v^0_{no})} v^{0^j}_{no}(t)\, f^j_{v^0_{no}}(x,y)\right)$$

$$\vdots$$

$$\tilde{\psi}_{3y} = \sum_{no=1}^{Nne} \mathbb{N}^e_{no}(x,y)\left(\psi_{3y_{no}}(t) + \sum_{j=1}^{nf(\psi_{3y_{no}})} \psi^j_{3y_{no}}(t)\, f^j_{\psi_{3y_{no}}}(x,y)\right) \tag{24}$$

where $\mathbb{N}^e_{no}(x,y)$ is the portion of the PoU functions matrix related to the node no, Nne stands for the number of nodes and $nf(\bullet_{no})$ denotes the number of enrichment functions associated with the unknown $\bullet$ at node no. Hence, by assembling all the functions in a single matrix of displacement approximations, one has a symbolic representation for the discretized unknown fields, whose matrix $\mathbf{N}^e$ has dimensions $7 \times 7(Nne + npar)$, with $npar$ equal to the number of enrichment parameters of the element.

The electric potential approximation in the coplanar directions (x, y), in any position within a piezoelectric ply k, according to the GFEM methodology, is built with the same PoU functions, $\mathbb{N}^e_{no}(x,y)$, used to approximate the mechanical displacement fields. The approximation $\tilde{\varphi}(\mathbf{x},t)^{k^e}$ is expressed by

$$\tilde{\varphi}(\mathbf{x},t)^{k^e} = \sum_{no=1}^{Nne} \mathbb{N}^e_{no}(x,y) \times \left(\varphi^k_{no}(z,t) + \sum_{j=1}^{nf(\varphi^k_{no})} \varphi^{k^j}_{no}(z,t)\, f^j_{\varphi^k_{no}}(x,y)\right). \tag{25}$$

Replacing (22) in (25) one obtains

$$\tilde{\varphi}(\mathbf{x},t)^{k^e} = \sum_{no=1}^{Nne} \mathbb{N}^e_{no}(x,y)\left\{[\varphi^{k-1}_{no}(t)\zeta_{k-1} + \varphi^k_{no}(t)\zeta_k] + \sum_{j=1}^{nf(\varphi^k_{no})} [\varphi^{k-1^j}_{no}(t)\zeta_{k-1} + \varphi^{k^j}_{no}(t)\zeta_k] f^j_{\varphi^k_{no}}(x,y)\right\}. \tag{26}$$

All degrees of freedom involving electric and mechanical unknowns are grouped in the following way, in a vector of nodal parameters in the element, associated with node no

$$\mathbb{U}^{e^{\mathrm{T}}}_{no} = \Big\{\ldots, u^0_{no}, u^{0^1}_{no}, \ldots, u^{0^{nf(u^0_{no})}}_{no}, v^0_{no}, v^{0^1}_{no}, \ldots, v^{0^{nf(v^0_{no})}}_{no}, w^0_{no}, w^{0^1}_{no}, \ldots, w^{0^{nf(w^0_{no})}}_{no}, \ldots, \psi_{3y_{no}}, \psi^1_{3y_{no}}, \ldots, \psi^{nf(\psi_{3y_{no}})}_{3y_{no}}, \varphi^1_{no}, \varphi^{1^1}_{no}, \ldots, \varphi^{1^{nf(\varphi^1_{no})}}_{no}, \varphi^2_{no}, \varphi^{2^1}_{no}, \ldots, \varphi^{2^{nf(\varphi^2_{no})}}_{no}, \ldots \ldots, \varphi^N_{no}, \varphi^{N^1}_{no}, \ldots, \varphi^{N^{nf(\varphi^N_{no})}}_{no}, \ldots\Big\}. \tag{27}$$

The extensional, flexural and warp strains can be grouped in a vector $\boldsymbol{\varepsilon}_{mf}$ such that

$$\boldsymbol{\varepsilon}_{mf} = \begin{Bmatrix} \boldsymbol{\varepsilon}^0 \\ \boldsymbol{\kappa}_1 \\ \boldsymbol{\kappa}_3 \end{Bmatrix}. \tag{28}$$

In this way, the approximation of the coplanar strains over an arbitrary element e is accomplished by substituting (24) into (18)

$$\tilde{\boldsymbol{\varepsilon}}(\mathbf{x},t)^e = \sum_{no=1}^{Nne} \mathbb{B}^e_{mf_{no}}(x,y)\mathbb{U}^e_{no}(t) = \mathbf{B}^e_{mf}\mathbf{U}^e. \tag{29}$$

This provides the *in-plane strains approximation matrix*, $\mathbf{B}^e_{mf}$, of dimensions $9 \times 7(Nne + npar)$, following the proposed organization shown in (28), whose portion related to the node no, $\mathbb{B}^e_{mf_{no}}$, is written in the form

$$\mathbb{B}^e_{mf_{no}} = \begin{bmatrix} \frac{\partial N_{no}}{\partial x} & \frac{\partial}{\partial x}(\Lambda^1_{u^0_{no}}) & \cdots & \frac{\partial}{\partial x}(\Lambda^{nf(u^0_{no})}_{u^0_{no}}) \\ 0 & 0 & \cdots & 0 \\ \cdots \frac{\partial N_{no}}{\partial y} & \frac{\partial}{\partial y}(\Lambda^1_{u^0_{no}}) & \cdots & \frac{\partial}{\partial y}(\Lambda^{nf(u^0_{no})}_{u^0_{no}}) \\ \vdots & \vdots & \cdots & \vdots \\ 0 & 0 & \cdots & 0 \end{bmatrix}$$

$$\begin{matrix} 0 & 0 & \cdots & 0 & \cdots \\ \frac{\partial N_{no}}{\partial y} & \frac{\partial}{\partial y}(\Lambda^1_{v^0_{no}}) & \cdots & \frac{\partial}{\partial y}(\Lambda^{nf(v^0_{no})}_{v^0_{no}}) & \cdots \\ \frac{\partial N_{no}}{\partial x} & \frac{\partial}{\partial x}(\Lambda^1_{v^0_{no}}) & \cdots & \frac{\partial}{\partial x}(\Lambda^{nf(v^0_{no})}_{v^0_{no}}) & \cdots \\ \vdots & \vdots & \cdots & \vdots & \ddots \\ 0 & 0 & \cdots & 0 & \cdots \end{matrix}$$

$$\begin{matrix} & & & & \overbrace{\qquad\qquad}^{2\times\sum_{\varrho}(1+nf(\varphi^{\varrho}_{no}))} \\ \cdots & 0 & 0 & \cdots & 0 & 0 \cdots 0 \\ \cdots & 0 & 0 & \cdots & 0 & 0 \cdots 0 \\ \cdots & 0 & 0 & \cdots & 0 & 0 \cdots 0 \\ \ddots & \vdots & \vdots & \cdots & \vdots & \vdots \cdots \vdots \\ \cdots & \frac{\partial N_{no}}{\partial x} & \frac{\partial}{\partial x}(\Lambda^1_{\psi_{3y_{no}}}) & \cdots & \frac{\partial}{\partial x}(\Lambda^{nf(\psi_{3y_{no}})}_{\psi_{3y_{no}}}) & 0 \cdots 0 \end{matrix} \quad \cdots \Bigg] \tag{30}$$

where $\Lambda^{\circ}_{\bullet} = N_{no}(x,y) f^{\circ}_{\bullet}(x,y)$ for the unknown $\bullet$ of the node, $\circ$ is the order of the enrichment function and $1 \leqslant \varrho \leqslant n_{\mathrm{piez}}$.

Similarly, the transverse shear strains can be grouped as

$$\boldsymbol{\gamma}_c = \begin{Bmatrix} \boldsymbol{\gamma}^0 \\ 3\boldsymbol{\kappa}_2 \end{Bmatrix}. \tag{31}$$

These strains are approximated over an element e by substituting (24) into (20)

$$\tilde{\boldsymbol{\gamma}}_c(\mathbf{x},t)^e = \sum_{no=1}^{Nne} \mathbb{B}^e_{c_{no}}(x,y)\mathbb{U}^e_{no}(t) = \mathbf{B}^e_c\mathbf{U}^e \tag{32}$$

leading to the *transverse shear approximation matrix*, $\mathbf{B}^e_c$, of dimensions $4 \times 7(Nne + npar)$, following the proposed organization shown in (31) and (30).

The electric field vector $\mathbf{E}(\mathbf{x},t)$ is defined as the negative gradient of the electric potential function, such that

$$\mathbf{E}(\mathbf{x},t) = -\nabla\varphi(\mathbf{x},t) = \begin{Bmatrix} E_x \\ E_y \\ E_z \end{Bmatrix} = \begin{Bmatrix} -\frac{\partial\varphi(\mathbf{x},t)}{\partial x} \\ -\frac{\partial\varphi(\mathbf{x},t)}{\partial y} \\ -\frac{\partial\varphi(\mathbf{x},t)}{\partial z} \end{Bmatrix}. \tag{33}$$

Then, using the definition of $\tilde{\varphi}(\mathbf{x}, t)^{k^e}$ in (26), it is possible to express the electric field approximation over an element e, within a piezoelectric ply k, by

$$\tilde{\mathbf{E}}(\mathbf{x}, t)^{k^e} = -\sum_{no=1}^{Nne} \begin{Bmatrix} \frac{\partial}{\partial x}\{\mathbb{N}^e_{no}(x, y)[\varphi^{k-1}_{no}(t)\zeta_{k-1} + \varphi^{k}_{no}(t)\zeta k]\} \\ \frac{\partial}{\partial y}\{\mathbb{N}^e_{no}(x, y)[\varphi^{k-1}_{no}(t)\zeta_{k-1} + \varphi^{k}_{no}(t)\zeta_{k}]\} \\ \frac{\partial}{\partial z}\{\mathbb{N}^e_{no}(x, y)[\varphi^{k-1}_{no}(t)\zeta_{k-1} + \varphi^{k}_{no}(t)\zeta_{k}]\} \end{Bmatrix}. \quad (34)$$

Finally, the electric field vector within a piezoelectric ply k can be approximated in the form

$$\tilde{\mathbf{E}}(\mathbf{x}, t)^{k^e} = -\sum_{no=1}^{Nne} \mathbb{B}^{k^e}_{no}\mathbb{U}^e_{no} = -\mathbf{B}^{k^e}\mathbf{U}^e. \quad (35)$$

This equation provides the *electric field approximation matrix* within a piezoelectric ply k, $\mathbf{B}^{k^e}$, of dimensions $3 \times 7(Nne + npar)$, following the proposed organization shown in (33), where the portion related to the node no, $\mathbb{B}^{k^e}_{no}$, is given by

$$\mathbb{B}^{k^e}_{no} = \begin{bmatrix} \overbrace{\begin{matrix} 0 & \cdots & 0 & 0 & \cdots & 0 \\ \cdots 0 & \cdots & 0 & 0 & \cdots & 0 \\ 0 & \cdots & 0 & 0 & \cdots & 0 \end{matrix}}^{7+nf(u^0_{no})+\cdots+nf(\psi_{3\gamma no})} \\ \\ \end{bmatrix}$$

$$\begin{bmatrix} \overbrace{\begin{matrix} 0 & \cdots & 0 \\ 0 & \cdots & 0 \\ 0 & \cdots & 0 \end{matrix}}^{2\times\sum_{\varrho_k}(1+nf(\varphi^{\varrho_k}_{no}))} & \zeta_{k-1}\frac{\partial N_{no}}{\partial x} & \zeta_{k-1}\frac{\partial}{\partial x}(\Lambda^{1}_{\varphi^{k-1}_{no}}) & \cdots \\ & \zeta_{k-1}\frac{\partial N_{no}}{\partial y} & \zeta_{k-1}\frac{\partial}{\partial y}(\Lambda^{1}_{\varphi^{k-1}_{no}}) & \cdots \\ & -\frac{1}{h_k}N_{no} & -\frac{1}{h_k}(\Lambda^{1}_{\varphi^{k-1}_{no}}) & \cdots \\ \zeta_{k-1}\frac{\partial}{\partial x}(\Lambda^{nf(\varphi^{k-1}_{no})}_{\varphi^{k-1}_{no}}) & \zeta_k\frac{\partial N_{no}}{\partial x} & \zeta_k\frac{\partial}{\partial x}(\Lambda^{1}_{\varphi^{k}_{no}}) & \\ \zeta_{k-1}\frac{\partial}{\partial y}(\Lambda^{nf(\varphi^{k-1}_{no})}_{\varphi^{k-1}_{no}}) & \zeta_k\frac{\partial N_{no}}{\partial y} & \zeta_k\frac{\partial}{\partial y}(\Lambda^{1}_{\varphi^{k}_{no}}) & \\ -\frac{1}{h_k}(\Lambda^{nf(\varphi^{k-1}_{no})}_{\varphi^{k-1}_{no}}) & \frac{1}{h_k}N_{no} & \frac{1}{h_k}(\partial\Lambda^{1}_{\varphi^{k}_{no}}) & \end{bmatrix}$$

$$\begin{bmatrix} \cdots & \zeta_k\frac{\partial}{\partial x}(\Lambda^{nf(\varphi^{k}_{no})}_{\varphi^{k}_{no}}) & \overbrace{\begin{matrix} 0 & \cdots & 0 \\ 0 & \cdots & 0 \\ 0 & \cdots & 0 \end{matrix}}^{2\times\sum_{\varrho^k}(1+nf(\varphi^{\varrho^k}_{no}))} \\ \cdots & \zeta_k\frac{\partial}{\partial y}(\Lambda^{nf(\varphi^{k}_{no})}_{\varphi^{k}_{no}}) & \cdots \\ \cdots & \frac{1}{h_k}(\Lambda^{nf(\varphi^{k}_{no})}_{\varphi^{k}_{no}}) & \end{bmatrix} \quad (36)$$

with $1 \leqslant \varrho_k \leqslant (k-1)$ and $(k+1) \leqslant \varrho^k \leqslant (n_{\text{piez}} - k)$ and considering the piezoelectric layers to be noncontiguous and the same degree of enrichment for both surfaces of each piezoelectric layer k.

Developing each portion of the Hamilton's principle functional and inserting the variable discretizations we get the expression for the element contributions as follows. From the variation of potential energy it is possible to identify the purely mechanical stiffness, composed by a membrane-bending matrix, $\mathbf{K}^e_{mf}$, and transverse shear $\mathbf{K}^e_c$ matrix, whose integrations over the midplane domain lead to the following representations

$$\mathbf{K}^e_{mf} = \int_{\Omega_e} \mathbf{B}^{e^{\mathrm{T}}}_{mf} \begin{bmatrix} \mathbf{A} & \mathbf{B} & \mathbf{L} \\ \mathbf{B} & \mathbf{D} & \mathbf{F} \\ \mathbf{L} & \mathbf{F} & \mathbf{H} \end{bmatrix} \mathbf{B}^e_{mf}\, \mathrm{d}\Omega_e \quad (37)$$

$$\mathbf{K}^e_c = \int_{\Omega_e} \mathbf{B}^{e^{\mathrm{T}}}_{c} \begin{bmatrix} \mathbf{A}_c & \mathbf{D}_c \\ \mathbf{D}_c & \mathbf{F}_c \end{bmatrix} \mathbf{B}^e_{c}\, \mathrm{d}\Omega_e. \quad (38)$$

The sub-matrices $\mathbf{A}$, $\mathbf{B}$, $\mathbf{D}$, $\mathbf{F}$, $\mathbf{H}$ and $\mathbf{L}$ are components of the purely mechanical constitutive matrix of the membrane and bending of the laminate, of dimensions 9×9, and the sub-matrices $\mathbf{A}_c$, $\mathbf{D}_c$, $\mathbf{F}_c$, are the components of the purely mechanical constitutive matrix of transverse shear of the laminate. These matrix components are obtained by integration along the thickness in the following way

$$\{A_{ij}, B_{ij}, D_{ij}, L_{ij}, F_{ij}, H_{ij}\} = \sum_{k=1}^{N}\int_{z_{k-1}}^{z_k} C^k_{ij}\{1, z, z^2, z^3, z^4, z^6\}\, \mathrm{d}z \qquad i, j = 1, 2, 6. \quad (39)$$

$$\{A_{c_{ij}}, D_{c_{ij}}, F_{c_{ij}}\} = \sum_{k=1}^{N}\int_{z_{k-1}}^{z_k} C^k_{ij}\{1, z^2, z^4\}\, \mathrm{d}z \qquad i, j = 4, 5. \quad (40)$$

At this point it is convenient to decompose the electric field in each piezoelectric layer k into a constant and a linearly varying part along its thickness, in the form

$$\tilde{\mathbf{E}}^{k^e}(\mathbf{x}, t) = -\sum_{no=1}^{Nne}\{\mathbb{E}^{0k}_{no} + z\mathbb{E}^{1k}_{no}\} = -\{\mathbf{E}^{0k} + z\mathbf{E}^{1k}\}. \quad (41)$$

Similarly to the forms used for the deformation equations, (28) or (31), it is interesting to group the electric fields $\mathbf{E}^{0k}$ and $\mathbf{E}^{1k}$, in definition (41), in the following way

$$\tilde{\mathbf{E}}^{k^e} = -\begin{Bmatrix} \mathbf{E}^{0k} \\ \mathbf{E}^{1k} \end{Bmatrix}. \quad (42)$$

From the expression of the variation of strain energy, it is possible also to identify the coupled mechanical–electrical stiffness, composed of a membrane-bending coupled stiffness part $\mathbf{K}^e_{mf-\varphi}$ and a transverse shear coupled stiffness $\mathbf{K}^e_{c-\varphi}$, whose integration on the in-plane domain results in

$$\mathbf{K}^e_{mf-\varphi} = \int_{\Omega_e} \mathbf{B}^{e^{\mathrm{T}}}_{mf} \begin{bmatrix} \mathbf{O} & \mathbf{P} \\ \mathbf{P} & \mathbf{Q} \\ \mathbf{R} & \mathbf{S} \end{bmatrix}^{lam} \begin{bmatrix} \mathbf{E}^{1^e} \\ \vdots \\ \mathbf{E}^{n_{\text{piez}}{}^e} \end{bmatrix} \mathrm{d}\Omega_e \quad (43)$$

$$\mathbf{K}^e_{c-\varphi} = \int_{\Omega_e} \mathbf{B}^{e^{\mathrm{T}}}_{c} \begin{bmatrix} \mathbf{T} & \mathbf{U} \\ \mathbf{V} & \mathbf{W} \end{bmatrix}^{lam} \begin{bmatrix} \mathbf{E}^{1^e} \\ \vdots \\ \mathbf{E}^{n_{\text{piez}}{}^e} \end{bmatrix} \mathrm{d}\Omega_e. \quad (44)$$

The sub-matrices $\mathbf{O}^k$, $\mathbf{P}^k$, $\mathbf{Q}^k$, $\mathbf{R}^k$ and $\mathbf{S}^k$ are independents for each piezoelectric layer k, defining a mechanically electrically coupled constitutive matrix for membrane-bending of the laminate, of order $9 \times 6n_{\text{piez}}$, and the sub-matrices $\mathbf{T}^k$, $\mathbf{U}^k$, $\mathbf{V}^k$ and $\mathbf{W}^k$, defining a mechanically electrically coupled constitutive matrix for shear bending of the laminate, of order $4 \times 6n_{\text{piez}}$. Their components are given by

$$\{O^k_{ij}, P^k_{ij}, Q^k_{ij}, R^k_{ij}, S^k_{ij}\} = \int_{z_{k-1}}^{z_k} e^k_{ij}\{1, z, z^2, z^3, z^4\}\, \mathrm{d}z \qquad i, j = 1, 2, 6. \quad (45)$$

$$\{T^k_{ij}, U^k_{ij}, V^k_{ij}, W^k_{ij}\} = \int_{z_{k-1}}^{z_k} e^k_{ij}\{1, z, z^2, z^3\}\, \mathrm{d}z \qquad i, j = 4, 5. \quad (46)$$

The electrically mechanically coupled stiffness matrix, $\mathbf{K}^e_{\varphi u}$, is obtained by a similar procedure to that used for the mechanically electrically coupled stiffness matrix, $\mathbf{K}^e_{u\varphi}$. It should be noted that $\mathbf{K}^e_{\varphi u} = \mathbf{K}^{e^{\mathrm{T}}}_{u\varphi}$.

Finally, the purely electric stiffness matrix $\mathbf{K}^e_{\varphi\varphi}$ can be obtained by in-plane integration by

$$[\mathbf{K}^e_{\varphi\varphi}] = \int_{\Omega_e} \begin{bmatrix} \mathbf{E}^{1^e} \\ \vdots \\ \mathbf{E}^{n_{\mathrm{piez}}{}^e} \end{bmatrix}^{\mathrm{T}} \begin{bmatrix} \mathbf{X} & \mathbf{Y} \\ \mathbf{Y} & \mathbf{Z} \end{bmatrix}^{lam} \begin{bmatrix} \mathbf{E}^{1^e} \\ \vdots \\ \mathbf{E}^{n_{\mathrm{piez}}{}^e} \end{bmatrix} \mathrm{d}\Omega_e. \quad (47)$$

The purely electric constitutive matrix of the laminate is of order $6n_{\mathrm{piez}} \times 6n_{\mathrm{piez}}$ and it is formed by sub-matrices $\mathbf{X}^k$, $\mathbf{Y}^k$ and $\mathbf{Z}^k$, whose components are given by

$$\{X_{ij}, Y_{ij}, Z_{ij}\} = \int_{z_{k-1}}^{z_k} \chi^k_{ij}\{1, z, z^2\}\,\mathrm{d}z \qquad i, j = 1, 2, 3. \quad (48)$$

The total element stiffness matrix is obtained by adding all contributions

$$\mathbf{K}^e = \mathbf{K}^e_{uu} + \mathbf{K}^e_{u\varphi} + \mathbf{K}^e_{\varphi u} - \mathbf{K}^e_{\varphi\varphi}. \quad (49)$$

The element inertia matrix $\mathbf{M}^e$ is obtained by inserting the mechanical displacement approximation into the variation of kinetic energy and performing integration on the element midplane domain Ω_e. This results in

$$\mathbf{M}^e = \int_{\Omega_e} \mathbf{N}^{e^{\mathrm{T}}} \begin{bmatrix} \mathbf{P}_0 & \mathbf{P}_1 & \mathbf{P}_3 \\ \mathbf{P}_1 & \mathbf{P}_2 & \mathbf{P}_4 \\ \mathbf{P}_3 & \mathbf{P}_4 & \mathbf{P}_6 \end{bmatrix} \mathbf{N}^e \,\mathrm{d}\Omega_e \quad (50)$$

where $\mathbf{P}_0 = \rho_0 I_{3\times3}$, $\mathbf{P}_1 = \rho_1 I_{3\times2}$, $\mathbf{P}_2 = \rho_2 I_{2\times2}$, $\mathbf{P}_3 = \rho_3 I_{3\times2}$, $\mathbf{P}_4 = \rho_4 I_{2\times2}$ and $\mathbf{P}_6 = \rho_6 I_{2\times2}$. The Is are identity matrices or parts of them. The generalized masses are defined by

$$\{\rho_0, \rho_1, \rho_2, \rho_3, \rho_4, \rho_6\} = \sum_{k=1}^{N} \int_{z_{k-1}}^{z_k} \rho_k\{1, z, z^2, z^3, z^4, z^6\}\,\mathrm{d}z \quad (51)$$

where ρ_k is an equivalent mass per unit area of the layer k.

Similarly, the *vectors of equivalent nodal forces* are obtained from the variation of the external work, such that

$$\mathbf{F}^{e^V} = \int_{\Omega_e} \mathbf{N}^{e^{\mathrm{T}}}_{uu} \mathbf{N}^{f^e} F^V \,\mathrm{d}\Omega_e \qquad \mathbf{F}^{e^S} = \int_{\Omega_e} \mathbf{N}^{e^{\mathrm{T}}}_{uu} \mathbf{N}^{f^e} F^S \,\mathrm{d}\Omega_e$$
$$\mathbf{F}^{e^P} = \mathbf{N}^{e^{\mathrm{T}}}_{uu} F^P \qquad \mathbf{F}^{e^Q} = \int_{\Omega_e} \mathbf{N}^{e^{\mathrm{T}}}_{\varphi\varphi} \mathbf{N}^{q^e} Q^S \,\mathrm{d}\Omega_e \quad (52)$$

$\mathbf{N}^e_{uu}$ and $\mathbf{N}^e_{\varphi\varphi}$ are approximation arrays of the mechanical and electrical unknowns, respectively. The sum of all contributions results in the element nodal force vector $\mathbf{F}^e(t)$.

The semi-discrete algebraic equations of motion for the element are

$$\mathbf{M}^e \ddot{\mathbf{U}}^e(t) + \mathbf{K}^e \mathbf{U}^e(t) = \mathbf{F}^e(t). \quad (53)$$

In the particular case of a quasi-static problem the system becomes

$$\mathbf{K}^e \mathbf{U}^e = \mathbf{F}^e(t). \quad (54)$$

It is known that, even after the correct imposition of essential boundary conditions, the stiffness matrix shows a very high condition number, or becomes singular. This linear dependency between the system equations seems to occurs because the PoU and the enrichment functions are both polynomials. The algebraic solution must be obtained using a procedure appropriate for positive-semi-definite matrices. In this study, the iterative K–ε method of Babuška presented by Strouboulis *et al* (2000) is employed.

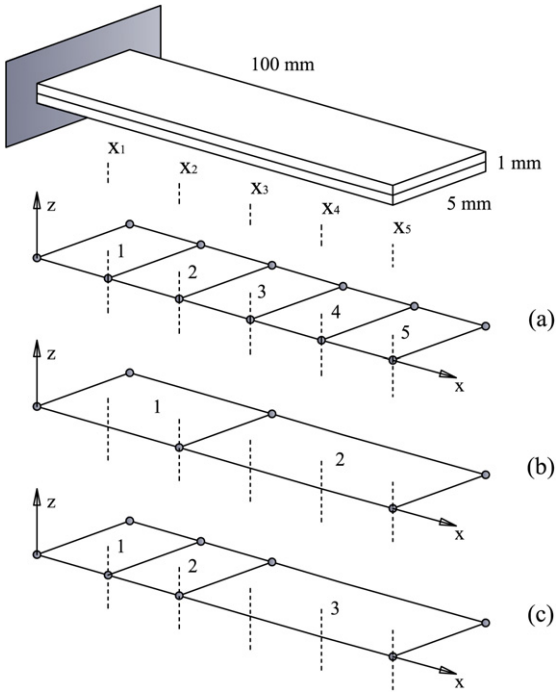

Figure 1. Piezoelectric bimorph beam and discretized models: (a) MEF mesh; (b) and (c) GFEM meshes.

5. Numerical examples

The proposed GFEM formulation was incorporated into a finite element code for validation. The numerical results generated from the following models were compared with published experimental and numerical results.

5.1. Case 1—bimorph plate as actuator

This problem consists of a bimorph working as an actuator. The top and bottom surfaces of the beam are subjected to electric potentials of 0.5 V and −0.5 V, respectively, resulting in a unitary electric field across the thickness of the beam, and the corresponding displacements are determined. This problem was subjected to experimental measurements obtained by Tzou and Tseng (1990). Their experimental apparatus consists of a cantilevered piezoelectric bimorph beam constructed of two layers of PVDF bonded together and polarized in opposite directions. The dimensions and discretized models used in the numerical analysis reported here are shown in figure 1. The material properties are given in table 1.

The experimental results obtained by Tzou and Tseng (1990) have been used to verify numerical results of several researchers, and some of these results are compared with those

Table 1. Material properties of the piezoelectric bimorph.

$E = 2$ GPa	$\nu = 0.29$
$e_{31} = 0.046$ C m^{-2}	$e_{32} = 0.046$ C m^{-2}
$\chi_{11} = \chi_{22} = \chi_{33} = 0.1062 \times 10^{-9}$ F m^{-1}	

obtained from the present formulation. These numerical results will be briefly commented on. Firstly, Hwang and Park (1993) considered a regular mesh with five linear plate elements whose formulation is based on the CLPT for mechanical displacements and endowed with one electric degree of freedom per piezoelectric layer per element, which means one equipotential surface within the element.

Detwiler *et al* (1995) analyzed the problem with a regular finite element mesh with five linear plate elements. The formulation is based on FSDT for mechanical behavior. The electric potential is approximated in each element by one degree of freedom in each piezoelectric layer, and it is taken as constant in the in-plane directions.

Cen *et al* (2002) modeled this problem with a formulation based on FSDT for mechanical behavior and layerwise theory for the electric potential. The mesh is regular with five linear plate elements.

Lim *et al* (2005) considered that the deformation of a piezoelectric actuator-embedded structure can be estimated by using the linear elastic thermal analogy, which equivalently replaces the piezoelectric strain with thermally induced strain. The authors analyzed the structure using the HEXA 8 finite element implemented in the MSC/NASTRAN.

Faria (2006) analyzed this model using a mesh with five serendipity biquadratic finite elements formulated according to an HSDT for the mechanical description and the layerwise theory for the electric potential interpolation.

The results obtained in this paper for the problem considered are obtained with a mesh with two generalized finite elements, according to figure 1(b). The functions are enriched with polynomials of first and second degrees.

The displacement boundary conditions at the clamped end are enforced by excluding the nodal coefficients corresponding to the PoU functions at the boundary and the coefficients of all enrichment functions which are not null on the Dirichlet boundary. The boundary conditions of the electric potential are applied imposing the voltage on the top and bottom degrees of freedom corresponding to PoU on all nodes of the mesh.

A sequence of equally spaced points is defined on the plate, with coordinates x_1 to x_5 and its the transverse displacements are listed in table 2, which also shows the number of degrees of freedom (dof) for each model. The values at x_2 and x_5 are directly obtained from the solution of the algebraic equilibrium system (54), and the values at x_1, x_3 and x_4 are obtained from post-processing of the results.

The electric loading may be understood as an equivalent bending moment applied at the free end of the beam, such that the displacement response can be well approximated by a second degree polynomial, as can be verified by the response obtained with our first degree enrichment, which is approximately equal to the response of the second degree enrichment.

Table 2. Deflection induced by a unitary electric field.

	Transverse displacement ($\times 10^{-7}$ m)					
Theory	$\mathbf{x}_1$	$\mathbf{x}_2$	$\mathbf{x}_3$	$\mathbf{x}_4$	$\mathbf{x}_5$	dof
Present (PoU)	0.0005	0.0009	0.0021	0.0032	0.0044	28
Present (first degree enrich.)	0.1705	0.5538	1.2390	2.2155	3.4512	96
Present (orthot. first degree enrich.)	0.1717	0.5520	1.2413	2.2092	3.4500	70
Present (second degree enrich.)	0.2820	0.5533	1.2380	2.2156	3.4514	210
Faria (2006)	0.1400	0.5500	1.2400	2.2100	3.4500	303
Cen *et al* (2002)	0.1380	0.5520	1.2420	2.2080	3.4500	66
Detwiler *et al* (1995)	0.1400	0.5500	2.1000	2.2100	3.4500	50
Lim *et al* (2005)	0.1380	0.5520	1.2420	2.2070	3.4500	180
Tzou (experiment)	—	—	—	—	3.1500	—

Moreover, the models can be compared in terms of computing time or number of unknowns. Thus, since the computing time of the results reported in the literature are unavailable we have considered that similar amounts of unknowns leads to similar computing times for the final system of equations. Therefore, it can be seen from the results of the orthotropic first degree enrichment, a strategy of different p-refinement only in the longitudinal direction, provides good values for the transverse displacements with a competitive number of degrees of freedom, compared to other models.

According to Detwiler *et al* (1995), the experimental value given for tip deflection is less than that of the others because of shear losses through the bonding layer of the piezoelectric layers, and this bonding is considered perfect in the theoretical and numerical formulations.

5.2. Case 2—bimorph plate as a sensor

This case consists of the same bimorph as in case 1, but here it functions as a sensor. A prescribed deflection is applied at its free end and the electric potentials on the surfaces are calculated. The meshes used in this paper have two and three generalized finite elements, according to figures 1(b) and (c). The functions are enriched with polynomials of degrees less than or equal to three and the results are shown in table 3.

It can be observed that the electric potential distribution along the beam is approximately linear, as was also observed by Chee (2000) and Faria (2006). For example, Faria (2006) observed an electric potential of 323 V at the clamped end using a mesh with 40 finite elements. The present formulation provides an electric potential of 325 V as a result for both GFEM meshes (figures 1(b) and (c)) even though some mesh dependence can be noted. This influence may indicate the need for other non-polynomial enrichment functions for the electric potential.

5.3. Case 3—patched plate

The second validation case is based on experiments conducted by Crawley and Lazarus (1991). The experiment consists of a cantilevered laminated composite plate of graphite/epoxy, with fifteen distributed pairs of $G-1195$ piezoelectric patches (PZT) bonded evenly to the top and bottom surfaces, with

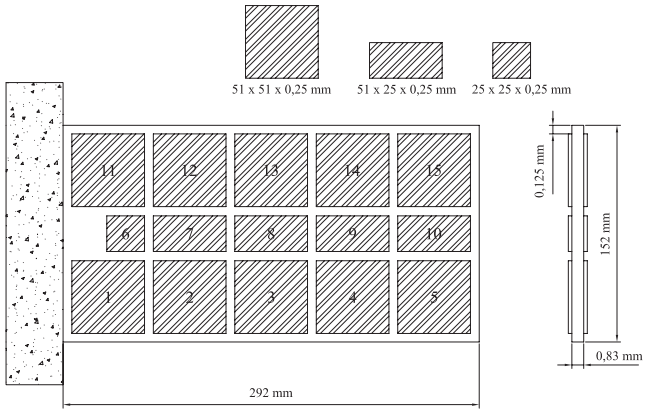

Figure 2. Cantilevered graphite/epoxy composite plate with distributed piezoelectric sensors and actuators.

Table 3. Electric potential induced by a deflection at the end.

	Electric potential (V)					
Theory	0	$\mathbf{x}_1$	$\mathbf{x}_2$	$\mathbf{x}_3$	$\mathbf{x}_4$	$\mathbf{x}_5$
Present (PoU) mesh b	369	259	148	99	49	0
Present (first degree enrich.) mesh b	245	211	176	160	144	128
Present (second degree enrich.) mesh b	325	260	196	131	65	0
Present (third degree enrich.) mesh b	325	261	196	131	66	0
Present (PoU) mesh c	356	373	82	48	14	−21
Present (first degree enrich.) mesh c	294	259	144	134	125	12
Present (second degree enrich.) mesh c	327	262	196	131	65	0
Present (third degree enrich.) mesh c	325	262	196	131	65	0
Faria (2006)	280	255	195	130	70	45
Detwiler *et al* (1995)	280	250	186	120	56	25
Hwang and Park (1993)	287	245	175	120	60	30

thickness 0.25 mm (see figure 2). Two laminates were tested: the first one with the stacking sequence $[0/45/-45]_s$, subjected to electric potentials of 100 and 157.6 V and the second one with the stacking sequence $[30/30/0]_s$ and subjected to an electric potential of 188.8 V, both with total thickness 0.83 mm.

Detwiler *et al* (1995) modeled the problem with a FSDT isoparametric quadrilateral finite element with a formulation based on an electric potential constant throughout the plane of the element.

Saravanos *et al* (1997) analyzed the problem using a completely layerwise description in a bilinear finite element formulation and considering a mesh with 16×9 finite elements. These authors used the following normalized form for the deflections, consistent with the way the experimental results were published

$$T_1 = \frac{w_2}{B} \qquad T_2 = \frac{1}{B}\left(w_2 - \frac{(w_1 + w_3)}{2}\right) \qquad T_3 = \frac{(w_3 - w_1)}{B} \tag{55}$$

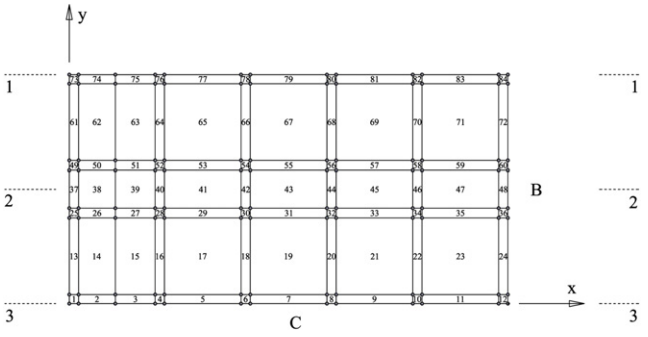

Figure 3. Mesh used in the GFEM model of the cantilevered composite plate.

where w_2, w_1 and w_3 are the transverse displacement along the midline and the two edges respectively, and B is the width of the plate. These three normalized displacements represent, or approximate, the axial bending deflection, the transverse bending curvature, and the twisting angle due to bending–twisting coupling, respectively. Furthermore, they considered a $[0/45/-45]_s$ lay-up cantilevered plate, whose deflection was induced applying a uniform electric field of 394 V mm^{-1}, of opposite polarity at the upper and lower piezoelectric patches.

Chee (2000), developed a formulation of piezoelectric plates considering HSDT and layerwise theory and implemented it using biquadratic serendipity finite elements. The author presents the solution for the T_1 displacement (55) from a model of this piezoelectric plate with a 12×7 finite element mesh and applying an uniform electric potential of 100 V for a $[0/45/-45]_s$ lay-up and 120 V for a $[30/30/0]_s$ lay-up.

Lee (2001) also used biquadratic serendipity finite elements formulated according to the layerwise theory, for both mechanical and electrical behaviors, and showed numerical T_1 results for this cantilevered composite plate modeled with a 16×9 finite element mesh. Two situations were analyzed: application of (a) a uniform electric field of 394 V mm^{-1} for a $[0/45/-45]_s$ lay-up and (b) a uniform electric field of 472 V mm^{-1} for a $[30/30/0]_s$ lay-up.

Faria (2006) also analyzed this problem using a mixed HSDT-LT formulation and considering a mesh with 12×7 biquadratic serendipity finite elements for both $[0/45/-45]_s$ and $[30/30/0]_s$ lay-ups subjected to uniform electric fields of 100 V and 120 V, respectively. This author also presented only the results for T_1 displacements.

The problem is solved with the present formulation considering the mesh shown in figure 3, using the PoU functions only, and isotropic enrichments of first and second degrees. The material properties are listed in table 4.

The displacement boundary conditions are applied in such a way that just the PoU and the enrichment functions which are not null on the Dirichlet boundary are eliminated. Hence, the contribution to the solution provided by the remaining enrichment functions is maintained on the clouds at this boundary. This procedure is easily implemented since the contours are straight lines and are parallel to the coordinate axis. The electric boundary conditions are applied imposing the voltage directly on the top and bottom electric degrees of freedom related to all elements with piezoelectric layers.

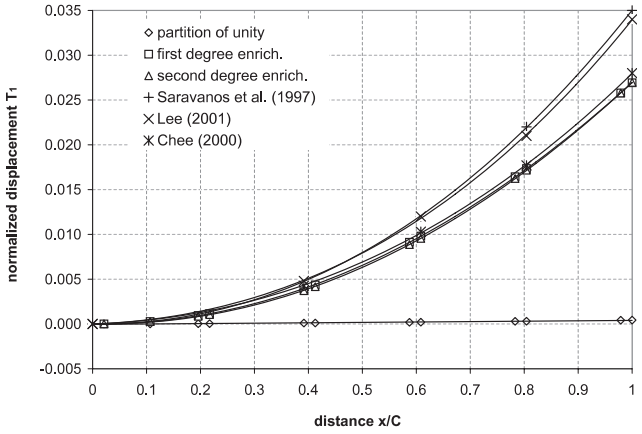

Figure 4. Longitudinal bending of a cantilevered $[0/45/-45]_s$ composite plate subjected to 100 V.

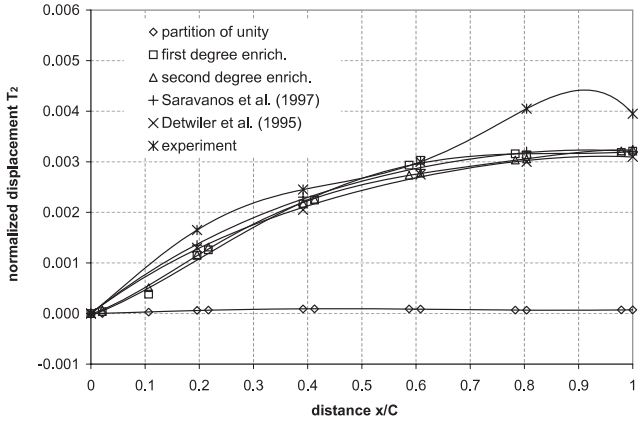

Figure 5. Transverse bending of a cantilevered $[0/45/-45]_s$ composite plate subjected to 157.6 V.

Table 4. Material properties.

Properties	Gr/epoxy	PZT-4
Elastic properties		
E_1 (N mm^{-2})	142.86×10^3	62.97×10^3
E_2 (N mm^{-2})	9.70×10^3	62.97×10^3
E_3 (N mm^{-2})	9.70×10^3	62.97×10^3
G_{12} (N mm^{-2})	6.00×10^3	24.20×10^3
G_{23} (N mm^{-2})	4.00×10^3	24.20×10^3
G_{13} (N mm^{-2})	6.00×10^3	24.20×10^3
ν_{12}	0.30	0.30
ν_{23}	0.37	0.30
ν_{31}	0.30	0.30
Piezoelectric coefficients		
e_{15} (C mm^{-2})	—	14.13×10^{-6}
e_{14} (C mm^{-2})	—	14.13×10^{-6}
e_{31} (C mm^{-2})	—	18.41×10^{-6}
e_{32} (C mm^{-2})	—	18.41×10^{-6}
e_{33} (C mm^{-2})	—	12.51×10^{-6}
Dielectric permittivity		
χ_{11} (F mm^{-1})	—	15.30×10^{-10}
χ_{22} (F mm^{-1})	—	15.30×10^{-10}
χ_{33} (F mm^{-1})	—	15.00×10^{-10}

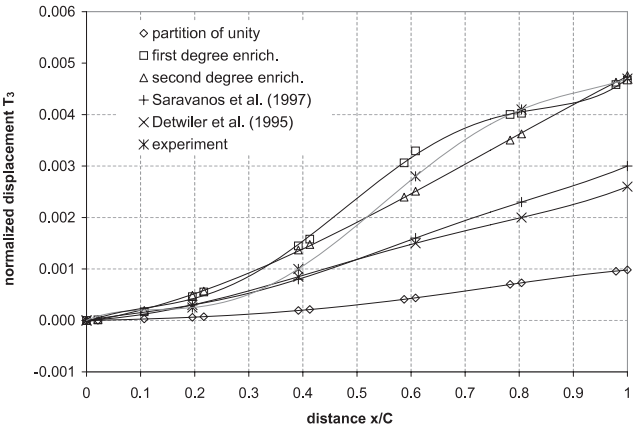

Figure 6. Twisting of a cantilevered $[0/45/-45]_s$ composite plate subjected to 157.6 V.

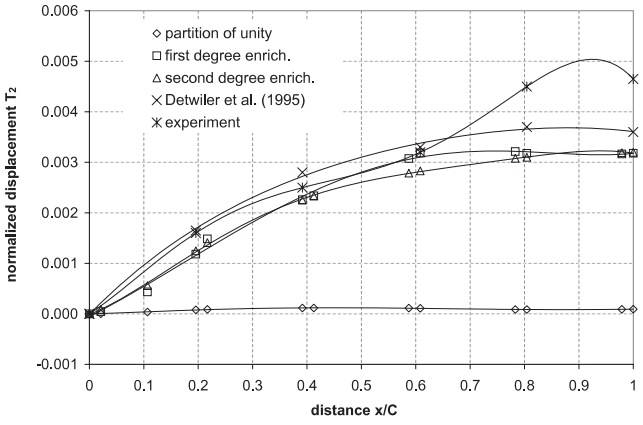

Figure 7. Transverse bending of a cantilevered $[30/30/0]_s$ composite plate subjected to 188.8 V.

Figure 4 shows the longitudinal bending (T_1) of the $[0/45/-45]_s$ plate subjected to 100 V and figures 5 and 6 show the transverse bending (T_2) and twisting (T_3), respectively, for the same lay-up and an electric potential of 157.6 V. Figures 7 and 8 also show the transverse bending and twisting, respectively, but for the $[30/30/0]_s$ plate, subjected to 188.8 V.

Figure 4 shows the convergence behavior of the solution for both first and second degree enrichments. The result reported by Faria (2006) is not included in the figure because the curve would be too close to that of the present formulation. The differences in the results obtained for the deflection at the end of plate in the present study and in those of Saravanos *et al* (1997) and by Lee (2001) are due to the differences in the mechanical kinematical hypothesis of each formulation. This is notable since the results for the present formulation and those of Chee (2000) differ only slightly, observing that the second polynomial degree provided by the serendipity finite elements of Chee (2000) and the first degree enrichment of the present are similar. Nevertheless, it should be pointed out that the GFEM formulation allows such a structure to be analyzed with

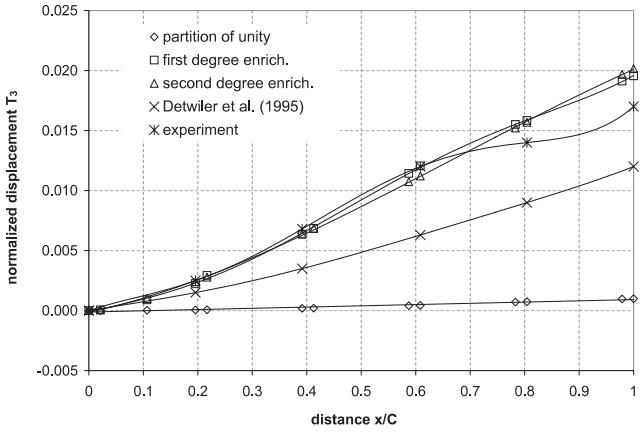

Figure 8. Twisting of a cantilevered $[30/30/0]_s$ composite plate subjected to 188.8 V.

the minimum amount of elements, according to the distribution of piezoelectric patches.

For the transverse bending, as shown in figures 5 and 7, the GFEM formulation shows good approximation capabilities as the enrichment degree increases. In addition, it is important to observe that the GFEM mesh requires the least number of elements and nodes possible for this distribution of piezoelectric patches.

For the twisting results, as shown in figures 6 and 8, the GFEM formulation shows more flexibility to reproduce the deformed shape compared to the results from the FSDT model of Detwiler *et al* (1995) and exhibit convergence behavior for the first and second degree enrichments.

6. Concluding remarks

The mixed layerwise-HSDT formulation for laminated plates with piezoelectric layers represents an efficient tool for modeling adaptive plate structures. The third degree expansion of mechanical displacements with piecewise linear discretization of the electric potential is a reasonable kinematic hypothesis for the phenomenon under analysis. The verification of the respective implementation was conducted through comparison with the results of several cases reported in the literature. The GFEM methodology for the enrichment of subspaces built with a conventional finite element partition of unity provides good approximation quality even when using a fixed finite element mesh. As the enrichment processes is from the partition of unity, through adding especial functions defined on global coordinates, the enrichment degree may vary over the connected domain without loss of conformity. This also leads to the possibility of enriching only some generalized unknowns or modeling problems with singularities. Such improvement may be seen for approximation of either primal or dual unknowns, logically limited by the hypothesis adopted for the physical modeling. The formulation is complete in the sense that it consistently considers the static as well as the dynamic behavior of adaptive plates. The performance in dynamic modeling will be the subject of a future publication.

Acknowledgments

D A F Torres gratefully acknowledges the financial support provided by the Brazilian government agency CAPES (Coordenação de Aperfeiçoamento de Pessoal de Nível Superior) during this research.

References

Allik H and Hughes T J R 1970 Finite element method for piezoelectric vibration *Int. J. Numer. Methods Eng.* **2** 151–8

Babuška I, Caloz G and Osborn J E 1994 Special finite element methods for a class of second order elliptic problems with rough coefficients *SIAM J. Numer. Anal.* **31** 945–81

Babuška I and Melenk J M 1997 The partition fo unity finite element method *Int. J. Numer. Methods Eng.* **40** 727–58

Barcellos C S, Mendonça P T R and Duarte C A 2009 A C^k continuous generalized finite element formulation applied to laminated Kirchhoff plate model *Comput. Mech.* **44** 377–93

Barros F B, Barcellos C S and Duarte C A 2007 $-p$ Adaptive C^k generalized finite element method for arbitrary polygonal clouds *Comput. Mech.* **41** 175–87

Cen S, Soh A-K, Long Y-Q and Yao Z-H 2002 A new 4-node quadrilateral FE model with variable electrical degrees of freedom for the analysis of piezoelectric laminated composite plates *Compos. Struct.* **58** 583–99

Chee C Y K 2000 Static shape control of laminated composite plate smart structure using piezoelectric actuators *PhD Thesis* University of Sydney

Chee C Y K, Tong L and Steven G P 1998 A review on the modeling of piezoelectric sensors and actuators incorporated in intelligent structures *J. Intell. Mater. Syst. Struct.* **9** 3–19

Cotoni V, Masson P and Côté F 2006 A finite element for piezoelectric multilayered plates: combined higher-order and piecewise linear C^0 formulation *J. Intell. Mater. Syst. Struct.* **17** 155–66

Crawley E F and Lazarus K B 1991 Induced strain actuation of isotropic and anisotropic plates *AIAA J.* **29** 944–51

Detwiler D T, Shen M-H H and Vankayya V B 1995 Finite element analysis of laminated composite structures containing distributed piezoelectric actuators and sensors *Finite Elements Anal. Des.* **20** 87–100

Duarte C A 1996 The hp-cloud method *PhD Thesis* The University of Texas at Austin

Duarte C A, Babuška I and Oden J T 2000 Generalized finite element method for three-dimensional structural mechanics problems *Comput. Struct.* **77** 215–32

Duarte C A, Hamzeh O N, Liszka T J and Tworzydlo W W 2001 A generalized finite element method for the simulation of three-dimensional crack propagation *Comput. Methods Appl. Mech. Eng.* **190** 2227–62

Duarte C A, Kim D-J and Quaresma D M 2006 Arbitrarily smooth generalized finite element approximations *Comput. Methods Appl. Mech. Eng.* **196** 33–56

Duarte C A and Oden J T 1996 An *h-p* adaptive method using cloud *Comput. Methods Appl. Mech. Eng.* **139** 237–62

Faria A W 2006 Finite element modeling of composite plates incorporating piezoelectric sensors and actuators: implementation and numerical assesssment *MSc Dissertation* Federal University of Uberlandia (abstract in English, text in Portuguese)

Gao J-X and Shen Y-P 2003 Active control of goemetrically nonlinear transient vibration of composite plates with piezoelectric actuators *J. Sound Vib.* **264** 911–28

Garcia O A 2003 Generalized finite elements in static analysis of plates and shells *PhD Thesis* Federal University of Santa Catarina (abstract in English, text in Portuguese)

Garcia O A, Fancello E A and Mendonça P T R 2009 Developments in the application of the generalized finite element method to thick shell problems *Comput. Mech.* **44** 669–82

Ha S K, Keilers C and Chang F K 1992 Finite element analysis of composite structures containing distributed piezoceramic sensors and actuators *AIAA J.* **30** 772–80

Hwang W S and Park H C 1993 Finite element modeling of piezoelectric sensors and actuators *AIAA J.* **31** 930–7

Lage R G, Soares C M M, Soares C A M and Reddy J N 2004 Layerwise partial mixed finite element analysis of magneto-electro-elastic plates *Comput. Struct.* **82** 1293–301

Lee H-J 2001 Finite element analysis of active and sensory thermopiezoelectric composite materials *Report 210892* Glenn Research Center—National Aeronautics and Space Administration

Levinson M 1980 An accurate simple theory of the statics and dynamics of elastic plates *Mech. Res. Commun.* **7** 343–50

Liew K M, He X Q, Tan M J and Lim H K 2004 Dynamic analysis of laminated composite plates with piezoelectric sensor/actuator patches using the FSDT mesh-free method *Int. J. Mech. Sci.* **46** 311–31

Lim S M, Lee S, Park H C, Yoon K J and Goo N S 2005 Design and demonstration of a biomimetic wing section using a lightweight piezo-composite actuator (LIPCA) *Smart Mater. Struct.* **14** 496–503

Melenk J M 1995 On generalized finite element method *PhD Thesis* University of Maryland

Melenk J M and Babuška I 1996 The partition of unity finite element method: basic theory and application *Comput. Methods Appl. Mech. Eng.* **139** 289–314

Oden J T, Duarte C A and Zienkiewicz O C 1998 A new cloud-based *hp* finite element method *Comput. Methods Appl. Mech. Eng.* **153** 117–26

Oden J T and Reddy J N 1976 *An Introduction to the Mathematical Theory of Finite Elements* (New York: Wiley)

O'Hara P J 2007 Finite element analysis of three-dimensional heat transfer for problems involving sharp thermal gradients *MSc Dissertation* University of Illinois at Urbana-Champaign

O'Hara P J, Duarte C A and Eason T 2009 Generalized finite element analysis of three-dimensional heat transfer problems exhibiting sharp thermal gradients *Comput. Methods Appl. Mech. Eng.* **198** 1857–71

Reddy J N 1999 On laminated composite plates with integrated sensors and actuators *Eng. Struct.* **21** 568–93

Reddy J N 2004 *Mechanics of Laminated Composite Plates and Shells: Theory and Analysis* (Boca Raton, FL: CRC Press)

Saravanos D A 1997 Mixed laminate theory and finite element for smart piezoelectric composite shell structures *AIAA J.* **35** 1327–33

Saravanos D A, Heyliger P R and Hopkins D A 1997 Layerwise mechanics and finite element for the dynamic analysis of piezoelectric composite plates *Int. J. Solids Struct.* **34** 359–78

Strouboulis T, Babuška I and Copps K 2000 The design and analysis of the generalized finite element method *Comput. Methods Appl. Mech. Eng.* **181** 43–69

Strouboulis T, Copps k and Babuška I 2001 The generalized finite element method *Comput. Methods Appl. Mech. Eng.* **190** 4081–193

Strouboulis T, Zhang L and Babuška I 2003 Generalized finite element method using mesh-based handbooks: application to problems in domains with many voids *Comput. Methods Appl. Mech. Eng.* **192** 3109–61

Szabó B and Babuška I 1991 *Finite Element Analysis* (New York: Wiley)

Tzou H S and Tseng C I 1990 Distributed piezoelectric sensor/actuator design for dynamic measurement/control of distributed parameter systems: a piezoelectric finite element approach *J. Sound Vib.* **138** 17–34